# Competition between antimagnetic and core rotation in $^{109}$Cd within covariant density functional theory

P. Zhang (张盼), B. Qi (亓斌), and S. Y. Wang (王守宇)*

*Shandong Provincial Key Laboratory of Optical Astronomy and Solar-Terrestrial Environment, School of Space Science and Physics, Shandong University, Weihai 264209, People's Republic of China*

(Received 22 January 2014; revised manuscript received 10 March 2014; published 4 April 2014)

The tilted axis cranking model based on covariant density functional theory is used to investigate the negative-parity yrast sequence in $^{109}$Cd. The energy spectra, the relation between spin and rotational frequency, deformation parameters, and reduced $E2$ transition probabilities are calculated, which are in good agreement with available data. The orientation of angular momentum is also extracted and discussed in detail. By investigating microscopically the orientation of angular momentum and the contributions of antimagnetic rotation and core rotation to the total angular momentum, we find that $^{109}$Cd should be a critical transitional nucleus between the antimagnetic and core rotations.

DOI: 10.1103/PhysRevC.89.047302 PACS number(s): 27.60.+j, 21.60.−n, 23.20.Lv, 21.10.Re

Since the prediction of antimagnetic rotation (AMR) in nuclei [1,2], this interesting phenomenon has attracted great attention. So far, firm experimental evidence of AMR has been reported in $^{105,106,107,108}$Cd [3–7], while $^{110}$Cd was suggested to exhibit a strong interplay between the antimagnetic and core rotations [8]. The odd-$A$ $^{109}$Cd nucleus discussed in this paper has been investigated by several experimental groups [9–12]. Chiara *et al.* [12] suggested the negative-parity yrast sequence of $^{109}$Cd was an AMR band based on the measured $\Im^2_{\rm tot}/B(E2) > 100\ \hbar^2\ {\rm MeV}^{-1}\ (e{\rm b})^{-2}$. On the other hand, Roy *et al.* [13] calculated the $I(\omega)$ plot and $B(E2)$ values of the negative-parity yrast sequence of $^{109}$Cd with Machiavelli's schematic semiclassical approach and compared these calculated results with the experimental data, which indicated that such sequences do not originate from the AMR. Therefore, it is interesting to investigate whether the negative-parity yrast sequence of $^{109}$Cd could be interpreted as the AMR. In this Brief Report, we employ the tilted axis cranking model based on covariant density functional theory (TAC-CDFT) to investigate the negative-parity yrast sequence of $^{109}$Cd in a fully self-consistent and microscopic way.

The TAC-CDFT with the point-coupling interaction was established in Ref. [14], which has succeeded in describing the AMR in $^{105}$Cd [15,16] and $^{112}$In [17]. In the TAC-CDFT, the equation of motion for the nucleons derived from the rotating Lagrangian is written as

$$[\boldsymbol{\alpha}\cdot(\boldsymbol{p}-\boldsymbol{V})+\beta(m+S)+V-\boldsymbol{\Omega}\cdot\hat{\boldsymbol{J}}]\psi_k=\epsilon_k\psi_k, \quad (1)$$

where $\hat{\boldsymbol{J}}=\hat{\boldsymbol{L}}+\frac{1}{2}\hat{\boldsymbol{\Sigma}}$ is the total angular momentum of the nucleon spinors, and the fields $S$ and $V^\mu$ are connected in a self-consistent way to the densities and current distributions. The solution of these equations yields single-particle energies, expectation values of three components $\langle J_i\rangle$ of the angular momentum, energy, quadrupole moments, $B(E2)$ transition probabilities, etc. Moreover, by taking into account the quantal corrections [18], the total angular momentum $J$ calculated corresponds to the quantum number of the angular momentum $I+1/2$ due to the approximation $J=\sqrt{I(I+1)}\approx I+1/2$. The detailed formulism can be found in Refs. [14,16,19–21].

The negative-parity yrast sequence of $^{109}$Cd has been observed up to the $\frac{51}{2}^-$ state, and is suggested to be built on the $\pi(g_{9/2})^{-2}\otimes\nu h_{11/2}$ configuration below the backbending and $\pi(g_{9/2})^{-2}\otimes\nu(h_{11/2})^3$ configuration above the backbending [11]. In our calculations, a basis of eight major oscillator shells is adopted. Moreover, the point-coupling interaction PC-PK1 [22] is used for the Lagrangian without any additional parameters, and pairing correlations are neglected. The calculated energy spectra $E(I)$ as a function of spin are presented in Fig. 1, together with the corresponding experimental data [11]. It is clear from Fig. 1 that the experimental energy spectra are well reproduced by the present TAC-CDFT calculations apart from the backbending region. Due to the level crossing, no converged solutions could be found in the backbending region (15–21 $\hbar$), where the calculated values are missing.

The calculated total angular momenta of the negative-parity yrast sequence in $^{109}$Cd are compared with the corresponding experimental values [11] as a function of rotational frequency in Fig. 2. As seen in Fig. 2, the experimental spin values are reproduced excellently below the backbending. Above the backbending, the calculated results overestimate the experimental values slightly. Moreover, the present TAC-CDFT calculations also support that the configuration changes from $\pi(g_{9/2})^{-2}\otimes\nu h_{11/2}$ to $\pi(g_{9/2})^{-2}\otimes\nu(h_{11/2})^3$ for the negative-parity yrast sequence in $^{109}$Cd.

We compare the calculated $B(E2)$ values and $\Im^{(2)}/B(E2)$ ratios with the available experimental data in Fig. 3. As shown in Figs. 3(a) and 3(b), the calculated $B(E2)$ values and $\Im^{(2)}/B(E2)$ ratios are in qualitative agreement with the available experimental data. It should be noted that the calculated $B(E2)$ values show a slight decrease with increasing spin above the backbending. While $B(E2)$ values below the backbending are almost constant. From Fig. 3(b), the calculated $\Im^{(2)}/B(E2)$ ratios exceed 100 ${\rm MeV}^{-1}\ (e{\rm b})^{-2}$, which is consistent with the expectation for a two-shear mechanism [2,23].

*sywang@sdu.edu.cn

 

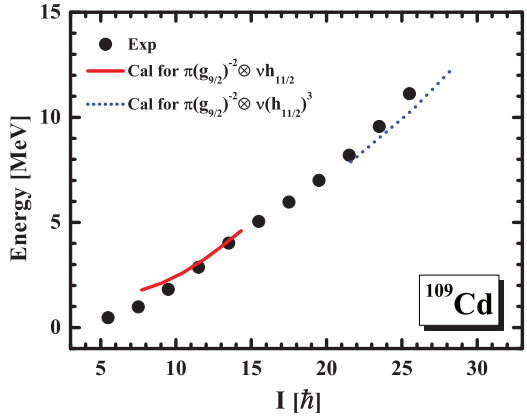


FIG. 1. (Color online) Energies $E(I)$ for the negative-parity yrast sequence in $^{109}$Cd calculated by the TAC-CDFT compared with the experimental data [11]. The energy at $I = 13.5\ \hbar$ is taken as reference.

In Fig. 4, we present the evolution of the deformation for the negative-parity yrast sequence in $^{109}$Cd in the $(\beta_2,\gamma)$ plane with increasing rotational frequency. As shown in Fig. 4, the $\beta_2$ values decrease from 0.195 to 0.185 as frequency increases from 0.2 to 0.6 MeV with the configuration of $\pi(g_{9/2})^{-2} \otimes \nu h_{11/2}$. Above the backbending, the $\beta_2$ values change from 0.209 to 0.167 as frequency increases from 0.5 to 0.8 MeV. It is worth noting that the calculated $\beta_2$ values are larger than 0.15, which implies that $^{109}$Cd is not a good case of the nearly spherical nucleus. We also find that the $\gamma$ values change from 14° to 1° as backbending occurs. This means that the negative-parity yrast sequence of $^{109}$Cd undergoes a shape change from a triaxial to a prolate one with the alignment of a pair of $h_{11/2}$ neutrons.

To examine the possible AMR mechanism of the negative-parity yrast sequence in $^{109}$Cd, the total angular momentum vectors of neutrons $(J_\nu)$ and the angular momentum vectors of two $g_{9/2}$ proton holes $(j_\pi)$ were calculated similarly as in Refs. [15,16]. The results for the $\pi(g_{9/2})^{-2} \otimes \nu h_{11/2}$ and $\pi(g_{9/2})^{-2} \otimes \nu(h_{11/2})^3$ configurations are presented in Figs. 5(a) and 5(b), respectively. It is clear from Fig. 5 that

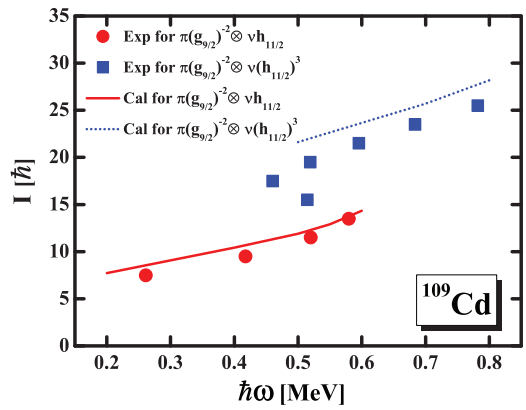


FIG. 2. (Color online) Total angular momentum as a function of the rotational frequency in the TAC-CDFT calculations for the configurations $\pi(g_{9/2})^{-2} \otimes \nu h_{11/2}$ and $\pi(g_{9/2})^{-2} \otimes \nu(h_{11/2})^3$ compared with the experimental data [11] for the negative-parity yrast sequence in $^{109}$Cd.

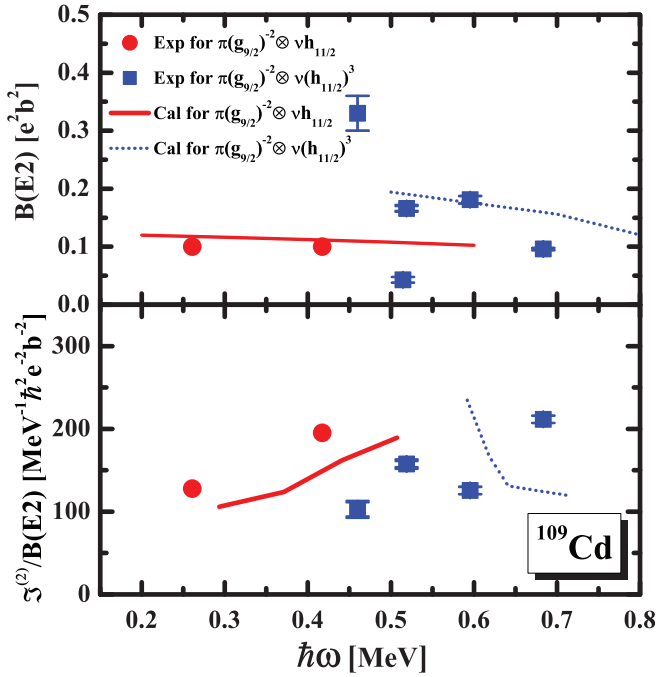


FIG. 3. (Color online) Calculated $B(E2)$ values and $\Im^{(2)}/B(E2)$ ratios for the $\pi(g_{9/2})^{-2} \otimes \nu h_{11/2}$ and $\pi(g_{9/2})^{-2} \otimes \nu(h_{11/2})^3$ bands in $^{109}$Cd compared with the experimental data [11].

the two proton angular momentum vectors are aligned back to back in opposite directions and are nearly perpendicular to the total angular momentum vectors of neutrons at the beginning frequency. As the rotational frequency increases, the vectors $j_\pi$ of the two $g_{9/2}$ proton holes align toward the vector $J_\nu$, the direction of the total angular momentum is almost unchanged. It presents a picture of the two shears closing simultaneously. The vectors $j_\pi$ and $J_\nu$ form the blades of the two shears.

As mentioned above, the calculated $\beta_2$ values indicated that $^{109}$Cd is not a good nearly spherical nucleus. Thus, the collective rotation of the core is also expected to contribute

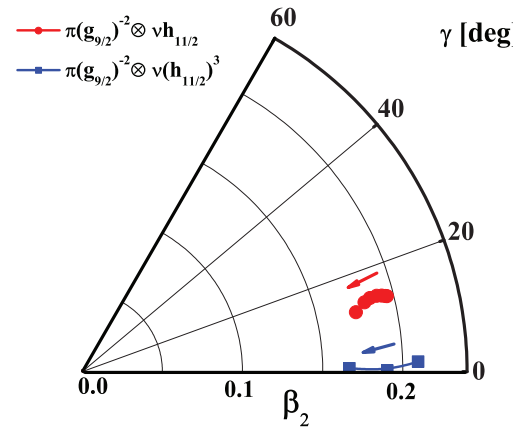


FIG. 4. (Color online) Evolutions of deformation in the $(\beta_2,\gamma)$ plane with rotational frequency in the TAC-CDFT calculations. The rotational frequencies increase from 0.15 to 0.60 MeV and from 0.50 to 0.80 MeV corresponding to the $\pi(g_{9/2})^{-2} \otimes \nu h_{11/2}$ and $\pi(g_{9/2})^{-2} \otimes \nu(h_{11/2})^3$ configurations, respectively.

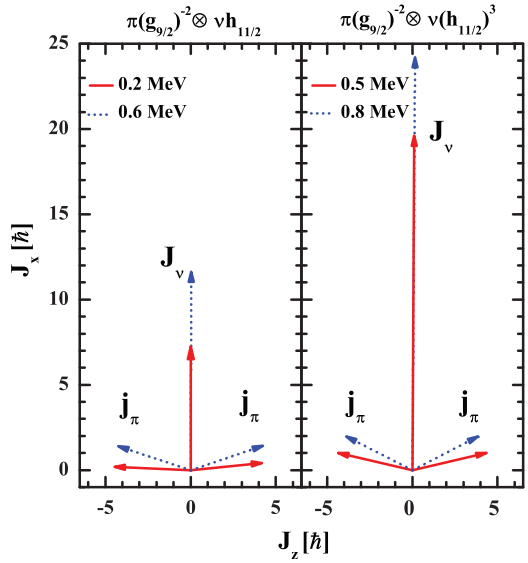


FIG. 5. (Color online) Angular momentum vectors of neutrons $J_\nu$ and the two $g_{9/2}$ proton holes $j_\pi$.

to the total angular momentum. However, in the TAC-CDFT calculation, all the energy and angular momentum come from individual nucleons and there is no inert core. Thus, the boundary of the contribution for these two modes (AMR and core) to angular momentum generation is difficult to identify. To investigate the proportion of the two modes in angular momentum generation, we used a simple picture to define AMR and core angular momentum. The angular momentum increment coming from $g_{9/2}$ proton holes and $h_{11/2}$ valence neutrons is defined as the contribution of the two-shear mechanism. The core angular momentum is defined by excluding the contributions of valence nucleons from the total angular momentum. We present the detailed contributions for these two modes to the angular momentum along $x$ axis ($j_x$) below and above the backbending in Table I. By this approach, the AMR contributes about 2.33 $\hbar$ when the rotational frequency increases from 0.2 to 0.6 MeV below the backbending, while the core contributes about 4.28 $\hbar$. With the rotational frequency increasing from 0.5 to 0.8 MeV above backbending, the AMR and the core contribute about 2.79 and 3.77 $\hbar$, respectively. Thereby, the contribution of AMR is about 35.3% (42.5%) of the total angular momentum increment below (above) the backbending. It means in $^{109}$Cd that the AMR mechanism, although very important, does not play a dominant role in the competition with the collective rotation of the core. As mentioned earlier, $^{110}$Cd ($N = 62$) was suggested to have a strong interplay between the antimagnetic and core rotations, while the other Cd isotopes for $N < 61$ were regarded as good candidates for AMR. Thus, $^{109}$Cd ($N = 61$) should be expected to be a critical transitional nucleus between the antimagnetic and core rotations. In addition, we find that the contribution of AMR above the backbending is larger than that below the backbending. It is consistent with the calculated results of $B(E2)$, i.e., the calculated $B(E2)$ values slightly decrease with increasing spin above the backbending. While $B(E2)$ values below the backbending are the almost constant. It should be noticed that our calculated results are different from those presented in Ref. [13]. It is mainly because the shears angle was evaluated artificially in Ref. [13]. All calculated results were influenced significantly by this shears angle. However, in the present microscopic calculation, the shears angle for a given rotational frequency is determined self-consistently by minimizing the total Routhian.

In summary, we use a fully self-consistent microscopic TAC-CDFT to investigate the negative-parity yrast sequence of $^{109}$Cd. The energy spectra, the relation between spin and rotational frequency, deformation parameters, and reduced $E2$ transition probabilities are calculated, which are in good agreement with available data. By investigating microscopically the orientation of the angular momentum and the contributions of AMR and core rotation to the total angular momentum, we find that $^{109}$Cd should be a critical transitional nucleus between the antimagnetic and core rotations.

The authors express sincere thanks to Prof. J. Meng, Prof. S. Q. Zhang, and Dr. P. W. Zhao for providing the TAC-CDFT code and the helpful suggestions. This work is supported by the National Natural Science Foundation (Grants No. 11175108 and No. 11005069), the Independent Innovation Foundation of Shandong University IIFSDU (No. 2013ZRYQ001), and the Graduate Innovation Foundation of Shandong University at WeiHai GIFSDUWH (No. yjs11031) of China. The computations were carried out on an HP Proliant DL785G6 server hosted by the Institute of Space Science of Shandong University.

TABLE I. Calculated angular momenta along the $x$ axis ($j_x$) for the AMR, core, and total angular momenta in the negative-parity yrast sequence of $^{109}$Cd.

| Configuration | | $j_x(\hbar)$ | | $\Delta j_x$ | Ratio |
|---|---|---|---|---|---|
| | | $\hbar\omega = 0.2$ MeV | $\hbar\omega = 0.6$ MeV | ($\hbar$) | (%) |
| $\pi(g_{9/2})^{-2} \otimes \nu h_{11/2}$ | AMR | 5.88 | 8.21 | 2.33 | 35.3 |
| | Core | 2.33 | 6.61 | 4.28 | 64.7 |
| | Total | 8.21 | 14.82 | 6.61 | |
| | | $\hbar\omega = 0.5$ MeV | $\hbar\omega = 0.8$ MeV | | |
| $\pi(g_{9/2})^{-2} \otimes \nu(h_{11/2})^3$ | AMR | 13.95 | 16.74 | 2.79 | 42.5 |
| | Core | 8.16 | 11.93 | 3.77 | 57.5 |
| | Total | 22.11 | 28.67 | 6.56 | |

[1] S. Frauendorf, Nucl. Phys. A **557**, 259 (1993).
[2] S. Frauendorf, Rev. Mod. Phys. **73**, 463 (2001).
[3] D. Choudhury *et al*., Phys. Rev. C **82**, 061308 (2010).
[4] A. J. Simons *et al*., Phys. Rev. Lett. **91**, 162501 (2003).
[5] D. Choudhury *et al*., Phys. Rev. C **87**, 034304 (2013).
[6] A. J. Simons *et al*., Phys. Rev. C **72**, 024318 (2005).
[7] P. Datta *et al*., Phys. Rev. C **71**, 041305 (2005).
[8] S. Roy *et al*., Phys. Lett. B **694**, 322 (2011).
[9] M. Meyer, R. Béraud, J. Danière, R. Rougny, J. Rivier, J. Tréherne, and D. Barnéoud, Phys. Rev. C **12**, 1858 (1975).
[10] S. Ohya, Y. Shida, O. Hashimoto, N. Yoshikawa, and M. Ishii, Nucl. Phys. A **325**, 408 (1979).
[11] S. Juutinen *et al*., Nucl. Phys. A **577**, 727 (1994).
[12] C. J. Chiara *et al*., Phys. Rev. C **61**, 034318 (2000).
[13] S. Roy and S. Chattopadhyay, Phys. Rev. C **83**, 024305 (2011).
[14] P. W. Zhao, S. Q. Zhang, J. Peng, H. Z. Liang, P. Ring, and J. Meng, Phys. Lett. B **699**, 181 (2011).
[15] P. W. Zhao, J. Peng, H. Z. Liang, P. Ring, and J. Meng, Phys. Rev. Lett. **107**, 122501 (2011).
[16] P. W. Zhao, J. Peng, H. Z. Liang, P. Ring, and J. Meng, Phys. Rev. C **85**, 054310 (2012).
[17] X. W. Li *et al*., Phys. Rev. C **86**, 057305 (2012).
[18] S. Frauendorf and J. Meng, Z. Phys. A **356**, 263 (1996).
[19] J. Peng, J. Meng, P. Ring, and S. Q. Zhang, Phys. Rev. C **78**, 024313 (2008).
[20] L. F. Yu, P. W. Zhao, S. Q. Zhang, P. Ring, and J. Meng, Phys. Rev. C **85**, 024318 (2012).
[21] J. Meng, J. Peng, S. Q. Zhang, and P. W. Zhao, Front. Phys. **8**, 55 (2013).
[22] P. W. Zhao, Z. P. Li, J. M. Yao, and J. Meng, Phys. Rev. C **82**, 054319 (2010).
[23] R. M. Clark and A. O. Macchiavelli, Annu. Rev. Nucl. Part. Sci **50**, 1 (2000).